

Analysis of the Transcript of the Herpes Simplex Virus DNA Polymerase Gene Provides Evidence that Polymerase Expression Is Inefficient at the Level of Translation

DORNE R. YAGER AND DONALD M. COEN*

Department of Biological Chemistry and Molecular Pharmacology, Harvard Medical School,
Boston, Massachusetts 02115

Received 16 November 1987/Accepted 23 February 1988

We have mapped the termini and determined the relative abundance and ribosome density of the major cytoplasmic transcript of the DNA polymerase (*pol*) gene of herpes simplex virus type 1. Nuclease protection and primer extension analyses located the 5' end of the major *pol* transcript at two closely spaced sites 51 and 57 nucleotides to the left of a *Bam*HI site at map position 0.413. S1-sensitive sites corresponding to additional minor transcripts were found to map further upstream within a palindromic sequence that contains a viral replication origin. The major 3' end was found to map 90 nucleotides upstream of a *Kpn*I site at map position 0.439. Quantitative S1 nuclease assays revealed that *pol* transcripts were nearly as abundant as transcripts encoded by the viral thymidine kinase gene. However, relatively few *pol* transcripts were found on large polyosomes at 5.5 h after infection, when *pol* transcripts were most abundant. This was in marked contrast to the polyribosome distribution of transcripts from the thymidine kinase gene and the major DNA-binding protein gene. These results and sequence features of the *pol* transcript suggest that *pol* expression is regulated, in part, at the level of translation.

The herpes simplex virus (HSV) genome is a 150-kilobase-pair (kbp) linear duplex DNA molecule that replicates in the nucleus of mammalian cells. Because HSV encodes a number of proteins that participate in viral DNA replication, it provides an excellent system for studying regulation of the expression of replication proteins. The central enzyme involved in HSV DNA replication is the virally encoded DNA polymerase (Pol). The *pol* gene has been mapped by marker rescue methods to a region minimally spanning 0.420 to 0.427 on the physical map (7, 8, 10). Northern (RNA) blot hybridization experiments demonstrated that one or more RNA species are transcribed left to right from this region (19). Nucleotide sequencing of this region revealed the presence of a 3,705-bp open reading frame, also oriented from left to right (Fig. 1), capable of encoding a polypeptide of approximately 136,000 daltons (14, 45). This is in rough agreement with previous size estimates of Pol (27, 43). However, no studies to date have demonstrated that this open reading frame is contained entirely within mRNA from the *pol* gene.

Like other HSV genes involved in nucleotide metabolism and DNA replication, such as those encoding thymidine kinase (*tk*) and the major DNA-binding protein, ICP8 (*dbp*), *pol* is expressed as an early or beta gene (19). The onset and overall rates of transcription of the *tk*, *dbp*, and *pol* genes are similar (11, 55). However, unlike the TK and DBP polypeptides, accumulation of radiolabeled Pol protein is not readily observed on protein gels (16, 17; Yager and Coen, unpublished results). This suggested that *pol* expression might be subject to regulation at a posttranscriptional level. This may have biological relevance, as other replicative polymerases are also relatively low-abundance polypeptides (2, 28, 33, 50).

As a prerequisite to addressing this question, we first mapped precisely the 5' and 3' ends of the *pol* transcript. Quantitative nuclease protection assays were then used to

determine the abundance of *pol* transcripts relative to other viral early transcripts and to determine the distribution of *pol* transcripts on polyribosomes. Our results, in combination with sequence features of the *pol* transcript, suggest that *pol* expression at peak times of *pol* transcript accumulation is inefficient at the level of translation.

MATERIALS AND METHODS

Cells and virus. African green monkey kidney (Vero) cells, grown in Dulbecco modified minimum essential medium supplemented with 4% fetal calf serum (56), and HSV type 1 strain KOS (48) were used.

Plasmid and viral DNA. Plasmid pSG17, containing the strain KOS *Eco*RI M fragment (coordinates 0.422 to 0.448), was a gift from R. Sandri-Goldin and M. Levine (15). Plasmid pKEF-P4, coordinates 0.357 to 0.422 (57), constructed by N. DeLuca, was generously provided by S. K. Weller. Plasmid and viral DNA were isolated as described (10).

Isolation of RNA. Cytoplasmic RNA was prepared from Vero cells at 5 h (except where noted) after mock infection or infection with a multiplicity of 10 PFU/cell. Cells were first washed and pelleted in ice-cold buffer (10 mM Tris hydrochloride [pH 7.9], 150 mM NaCl, 1.5 mM MgCl₂, 10 mM β-mercaptoethanol) and then lysed by addition of this buffer containing 0.5% Nonidet P-40 and 5 mM vanadyl ribonucleoside complex (Bethesda Research Laboratories, Inc.). Nuclei were removed by pelleting at 2,000 × g for 2 min. Cytoplasmic supernatants were incubated for 15 min at 37°C in 1% sodium dodecyl sulfate–25 mM EDTA–100 μg of proteinase K (Sigma Chemical Co.) per ml, phenol and chloroform extracted, and ethanol precipitated. The precipitated nucleic acid was suspended in 200 μl of 25 mM Tris hydrochloride (pH 7.5)–10 mM MgCl₂–500 mM NaCl–4 mM CaCl₂, digested with 20 μg of DNase I (Bethesda Research Laboratories) for 30 min at 37°C, extracted with equal volumes of phenol and chloroform, and precipitated with ethanol. The RNA precipitate was suspended in sterile

* Corresponding author.

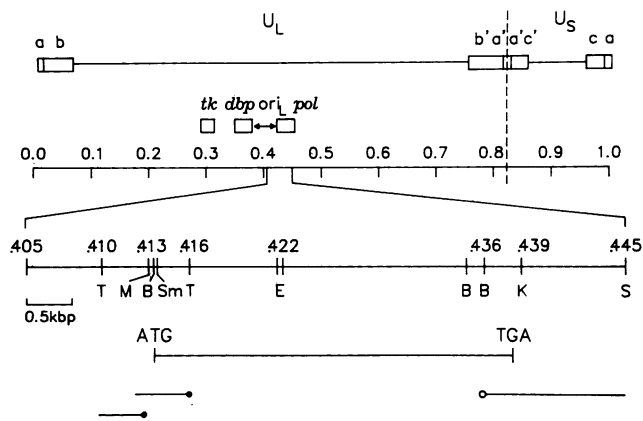


FIG. 1. HSV DNA probes used for mapping *pol* transcripts. The top lines show the arrangement of HSV genomic sequences, and a partial restriction map of HSV sequences used in mapping *pol* transcripts is shown. The approximate locations of *tk*, *dbp*, and *pol* (not to scale) are also depicted. The map position of the 1,235-amino-acid-coding major *pol* open reading frame is shown below the restriction map. The location of probes for primer extension and nuclease protection experiments are also depicted. Abbreviations: T, *Bst*EII; M, *Mae*III; Sm, *Sma*I; B, *Bam*HI; E, *Eco*RI; K, *Kpn*I; S, *Sal*I. 5'-End-labeled probes are represented by closed circles; those ending with open circles were 3'-end labeled. The radiolabeled fragment used for primer extension studies is indicated by the black square.

distilled water and quantitated by spectrophotometry and by ethidium bromide staining of samples electrophoresed in agarose gels.

Analysis of RNA structure and quantitation of viral mRNAs. End-labeled probes for nuclease mapping were prepared from plasmid and viral DNA fragments by standard protocols. Briefly, fragments for 5' mapping were dephosphorylated with calf intestinal phosphatase (Boehringer Mannheim Biochemicals) and subsequently labeled with [γ - 32 P]ATP (ICN; crude ATP, ca. 9,000 Ci/mmol) by using polynucleotide kinase (Boehringer Mannheim Biochemicals) (37). Fragments for 3' mapping were generated by labeling with Klenow fragment (Bethesda Research Laboratories) and [α - 32 P]deoxynucleoside triphosphates (ICN; ca. 3,000 Ci/mmol) (36). Virion and plasmid DNA fragments labeled at one end were then generated by digestion with a second restriction endonuclease and purified from agarose or polyacrylamide gels. Labeled DNA fragments were incubated with the indicated amounts of cytoplasmic RNA in 20 μ l of 80% recrystallized formamide–400 mM NaCl–40 mM HEPES [N-2-hydroxyethylpiperazine-*N,N'*-bis(2-ethanesulfonic acid) pH 6.4]–1 mM EDTA. Various amounts of DNA or RNA were used to demonstrate that the labeled probes were in molar excess to the hybridizing RNA species and to establish that the ensuing hybridization signal was directly proportional to the amount of RNA added. Hybridization with probes specific for the 5' end of *pol* mRNA were carried out for 5 h at 60°C. Because of their lower G+C content, hybridization to other probes was performed at 52°C. When hybridization to both *pol* and either the *tk* or *dbp* probe was required, hybridization was performed for 5 h at 60°C, followed by hybridization at 52°C for an additional 5 h. After hybridization, samples were diluted in 200 μ l of 280 mM NaCl–50 mM sodium acetate (pH 4.6)–4.5 mM ZnCl₂–20 μ g of single-stranded salmon testes DNA per ml and digested for 30 min at 37°C with 200 U of S1 nuclease

(Boehringer Mannheim Biochemicals). Reactions were terminated by phenol-chloroform extraction and ethanol precipitation. Nuclease-resistant material was resolved by electrophoresis on polyacrylamide gels containing 8 M urea and detected by direct autoradiography. Where appropriate, S1 digestion products were electrophoresed adjacent to a DNA sequence ladder (37) generated from the corresponding radiolabeled virion *Bam*HI-*Bst*EII fragment as described by Weller et al. (57). Relative levels of autoradiographic signals were quantitated by densitometric scanning of exposures of films that were within the linear range of a Schoeffel model SD3000 densitometer.

Digestion of hybridization reactions with exonuclease VII was performed in 200 μ l of 67 mM KPO₄ (pH 7.9)–8.3 mM sodium EDTA–10 mM β -mercaptoethanol–2 U of enzyme (Bethesda Research Laboratories) for 30 min at 37°C. Reaction products were desalted by Sephadex G-50 chromatography, ethanol precipitated, and resolved on polyacrylamide gels containing 8 M urea.

Primer extension mapping of the *pol* transcript was performed with total infected-cell RNA as described previously (11). The primer extension products were electrophoresed adjacent to radiolabeled *Msp*I fragments of pBR322.

Polyribosomes. Cells were incubated for 20 h prior to infection with 50 μ Ci of [3 H]uridine (38 Ci/mmol) per ml to prelabel rRNA. Labeled monolayers infected for 5.5 h were rinsed and then scraped into cold TKM buffer (50 mM Tris hydrochloride [pH 7.6], 100 mM KCl, 5 mM MgCl₂, 2 mM dithiothreitol, and 2.8 μ g of cycloheximide per ml). To lyse the cells, Nonidet P-40 was then added to a final concentration of 0.5%, and the mixture was incubated on ice for 5 min. Nuclei were pelleted by centrifugation at 2,000 \times g for 2 min at 4°C and then washed once with TKM buffer and repelleted. The two cytoplasmic supernatants from these centrifugations were pooled and brought to 1% sodium deoxycholate. Cytoplasmic supernatants representing 2 \times 10⁷ cells were layered onto 11-ml 15 to 50% sucrose gradients with a 0.5-ml cushion of 55% sucrose in TKM buffer containing 40 U of RNase inhibitor (Promega Biotec) per ml and centrifuged at 4°C in an SW40 rotor for 165 min at 35,000 rpm. Fractions (0.225 ml) were removed sequentially from the top of the gradients. Polysome profiles were monitored by determining the absorbance at 260 nm or by measuring the amount of radiolabeled RNA. Fractions were then pooled, extracted with phenol-chloroform, and ethanol precipitated prior to analysis.

RESULTS

Mapping the 5' end of the *pol* transcript. Figure 1 presents a partial restriction map of the region of the HSV genome containing the *pol* gene, showing the restriction sites that define the DNA fragments used in these experiments. To determine the approximate location of the 5' terminus of the *pol* transcript, a 550-bp *Mae*III-*Bst*EII DNA fragment (0.413 to 0.416) was 5'-end labeled at the *Bst*EII site, hybridized to infected-cell RNA, and then digested with S1 nuclease. The *Bst*EII site used is located 290 bp downstream from the initiation codon of the major *pol* open reading frame (14, 45). Infected-cell RNA protected a species of approximately 500 nucleotides (Fig. 2a, lanes 5 and 6). This observation places the major 5' S1-sensitive site to the left of the *Bam*HI site at 0.413. More full-length probe remained after hybridization with infected-cell RNA than with mock-infected-cell RNA, suggesting the presence of minor RNA species extending at least to the *Mae*III site (Fig. 2a, lanes 3, 5, and 6). Several

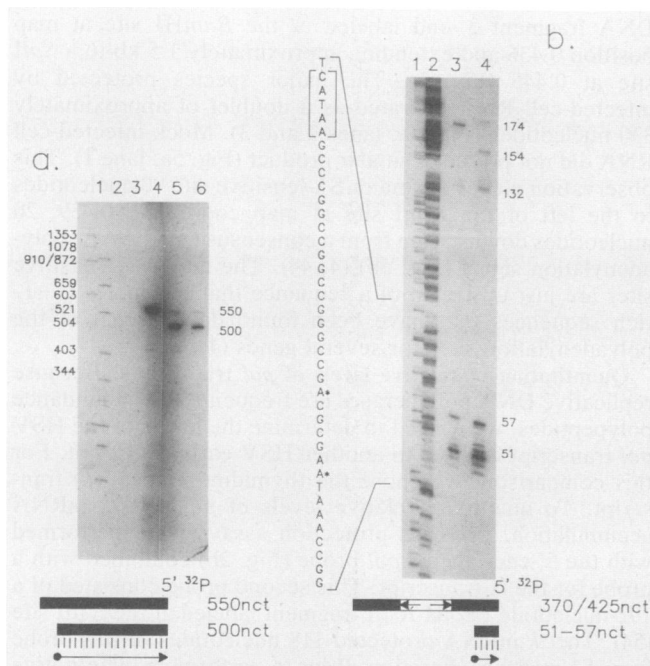


FIG. 2. Nuclease protection mapping of the 5' end of the major *pol* transcript. Cytoplasmic RNA isolated from Vero cells 6 h postinfection was hybridized to 5'-end-labeled probes for 5 h at 60°C. Hybridized mixtures were then digested with S1 nuclease. S1 nuclease-resistant products were resolved by electrophoresis in 6% acrylamide gels containing 8 M urea. (a) S1 mapping with a 550-bp *MaeIII-BstEII* fragment (0.413 to 0.416), labeled at the *BstEII* site. Lanes: 1 and 2, DNA size markers; 3, S1 nuclease-resistant products from 20 µg of mock-infected-cell RNA; 4, probe that was hybridized to mock-infected-cell RNA but not digested with S1 nuclease; 5, products from 20 µg of infected-cell RNA; 6, products from 10 µg of infected-cell RNA. The autoradiogram shown here was cut and spliced to remove an overexposed marker lane. (b) S1 nuclease mapping with a *BstEII-BamHI* fragment (0.410 to 0.413), labeled at the *BamHI* site. This region contains an origin of replication, *ori_L*, portions of which tend to undergo deletion events when cloned (50). Because of this, probes from both virion (425 nct) and plasmid (370 nct) sources were used. Lanes: 1, G sequence ladder of the transcript-coding strand of the virion DNA probe; 2, C and T sequence ladder; 3, products derived from 10 µg of infected-cell RNA and plasmid probe; 4, products derived from 10 µg of infected-cell RNA and virion probe. The location of the major S1-sensitive sites on the coding strand are indicated by asterisks, and are 51 and 57 nucleotides (nct) to the left of the *BamHI* site.

smaller species of low abundance were also protected, but could be ascribed mainly to protection of smaller probe fragments that arose spontaneously in these hybridization conditions (Fig. 2a, lane 4).

To map the major S1-protected species from the 5' end of the *pol* gene more precisely, S1 nuclease analysis was repeated with a DNA fragment 5'-end labeled at the *BamHI* (0.413) site and extending leftward to a *BstEII* site at 0.410 (Fig. 1). This region contains an HSV origin of replication, *ori_L*, and a perfect 144-nucleotide palindrome, portions of which often delete when cloned into conventional procaryotic vectors (57). To ensure that such deletions would not complicate mapping, probes from both virion (425 nucleotides) and plasmid pKEF-P4 (370 nucleotides) DNAs were used for S1 nuclease analysis. Comparison of S1 nuclease-resistant DNA fragments with a DNA sequence ladder generated from virion DNA 5' labeled at the *BamHI* site revealed that regardless of the probe source, the major 5' S1-sensitive

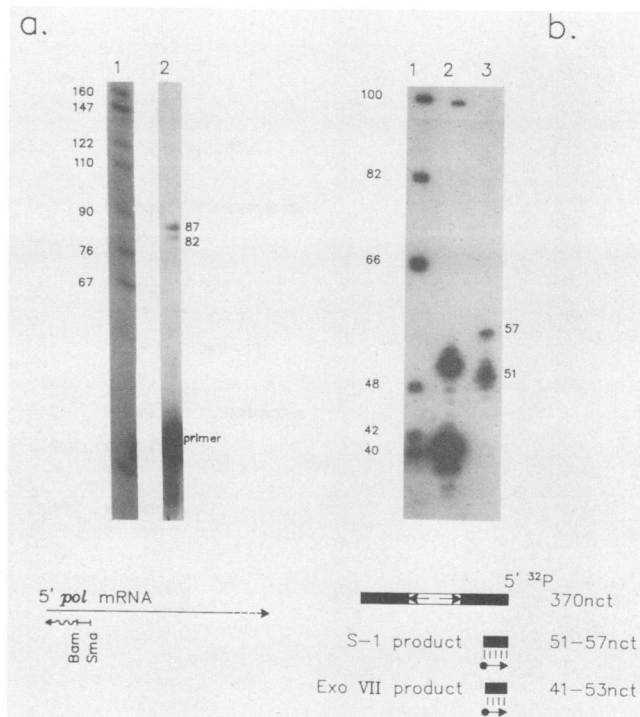


FIG. 3. Primer extension and exonuclease VII analysis. (a) Primer extension. Lane 1, DNA size markers; lane 2, primer extension products obtained with a 39-nucleotide (nct) *BamHI-SmaI* fragment (0.413) to prime infected-cell RNA templates. (b) Exonuclease VII analysis with the *BstEII-BamHI* fragment (0.410 to 0.413). Lanes: 1, ϕ X174 *HinI* markers; 2, exonuclease VII (Exo VII)-resistant products derived from 20 µg of infected-cell RNA; 3, S1 nuclease-resistant products derived from 20 µg of infected-cell RNA.

sites mapped to positions 51 and 57 nucleotides to the left of the *BamHI* site (Fig. 2b). These major sites lie approximately 55 and 60 nucleotides to the right of the palindrome. Minor sites further upstream were also detected.

To determine whether the major S1-sensitive sites correspond to the 5' terminus of the *pol* transcript, primer extension analysis was performed (11). The major extension products observed with a 39-nucleotide *BamHI-SmaI* fragment (mapping at 0.413) as a primer were approximately 82 and 87 nucleotides in length (Fig. 3a). These results place the 5' terminus of the *pol* transcript 48 and 53 nucleotides to the left of the *BamHI* site, in good agreement with the results obtained by nuclease protection analysis. Importantly, the primer extension products were no longer than would be predicted if the *pol* transcript 5' ends were defined by the 5' ends of the major S1-protected species. In addition, exonuclease VII digestion of RNA-DNA hybrids yielded two major protected products similar in size to those protected from S1 digestion (Fig. 3b). The slight difference in the sizes of the protected products is probably due to the removal of oligonucleotides by exonuclease VII, in contrast to S1 nuclease, which removes mononucleotides (9). We conclude that the S1-sensitive sites at 51 and 57 nucleotides to the left of the *BamHI* site represent the major 5' end of the *pol* transcript.

RNA species mapping to the *ori_L* palindrome. Species corresponding to sites lying within the *ori_L* palindrome were also protected by infected-cell RNA but not by mock-infected-cell RNA (Fig. 2b). These species represented less than 10% of the total amount of S1 nuclease-resistant material. To map these minor S1-sensitive sites precisely, sam-

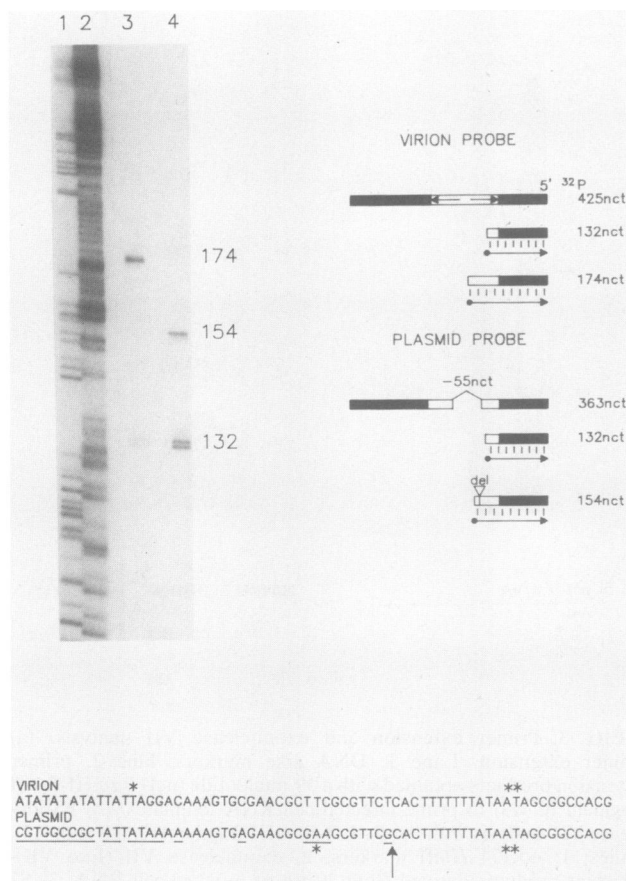


FIG. 4. Minor RNA species mapping to the *ori_L* palindrome. S1 nuclease analysis identical to that shown in Fig. 2b was repeated, but electrophoresis was prolonged to increase resolution of the minor products. To the right is a schematic drawing of the probes and their protected products. nct, Nucleotides. Below, the sequence position of the minor S1-sensitive sites are shown by asterisks, the arrow represents the position of the 55-bp deletion in pKEF-P4, and nucleotide mismatches between virion and plasmid DNAs are underlined.

ples identical to those shown in Fig. 2b were electrophoresed further (Fig. 4). The virion and plasmid probes each protected a species of 132 nucleotides, defining an S1-sensitive site between the major 5' end of the *pol* transcript and the deletion in pKEF-P4 (57; data not shown). The virion probe also protected a species of 174 nucleotides, defining an S1-sensitive site mapping within the deletion in pKEF-P4. The plasmid probe protected a species of similar abundance of 154 nucleotides. There was only a faint product of 144 nucleotides corresponding to the deletion junction. As depicted in Fig. 4, the upstream sequences that replace the deleted sequences of the plasmid are identical to the virion DNA sequence at six of the first seven nucleotides to the left of the deletion endpoint. We hypothesize that this accounts for the extension of this S1-resistant product.

Both of the minor S1-sensitive sites were found immediately upstream of A-G dinucleotides. Since we detected neither exonuclease VII nor primer extension products corresponding to these minor sites (data not shown), the possibility that these represent splice acceptor sites remains.

Mapping of the polyadenylation site of the *pol* transcript. The polyadenylation site of the *pol* transcript was located by S1 analysis of hybrids between infected-cell RNA and a

DNA fragment 3'-end labeled at the *Bam*HI site at map position 0.436 and extending approximately 1.5 kb to a *Sal*I site at 0.445 (Fig. 1). The major species protected by infected-cell RNA migrated as a doublet of approximately 330 nucleotides (Fig. 5a, lanes 2 and 3). Mock-infected-cell RNA did not protect a similar product (Fig. 5a, lane 1). This observation places the major S1-sensitive site 90 nucleotides to the left of the *Kpn*I site at map coordinate 0.439, 20 nucleotides downstream from a consensus (AATAAA) polyadenylation signal (Fig. 5b) (4, 44). The major S1-sensitive sites are just upstream of a sequence that resembles G+T-rich sequences that have been found downstream of the polyadenylation sites for several genes (4, 38).

Quantitation of relative levels of *pol* transcripts. Because replicative DNA polymerases are frequently low-abundance polypeptides, we wished to determine the levels of the HSV *pol* transcript relative to another HSV early transcript. For this comparison, we chose the thymidine kinase (*tk*) transcript. To quantitate relative levels of *pol* and *tk* mRNA accumulation, nuclease protection assays were performed with the 5'-end-labeled *pol* probe (Fig. 2b) combined with a probe for the *tk* transcript. This second probe consisted of a 192-nucleotide *Eco*RI-*Rsa*I fragment labeled at the *Rsa*I site (54). The *tk* mRNA protected 118 nucleotides of this probe from S1 nuclease digestion. Prior to performing quantitative comparisons of *pol* and *tk* mRNA levels, we determined that (i) the conditions used to detect the *pol* and *tk* transcripts simultaneously yielded signals similar to those obtained when each probe was used separately, (ii) neither probe generated radiolabeled species comigrating with species generated from the other, and (iii) the DNA probes were used at levels of molar excess (Fig. 6). Thus, the hybridization signals produced were linear with the amount of RNA present in each hybridization reaction (Fig. 6, compare lanes 2 and 3 and lanes 5 and 6).

Cytoplasmic RNA isolated at different times after infection was hybridized with a mixture of both probes and digested with S1 nuclease, and the products were resolved on a polyacrylamide gel (Fig. 7). The *pol* and *tk* probes were adjusted to the same specific activity, enabling direct comparison of *tk* and *pol* transcript levels. As shown in Fig. 7 and 8, the temporal patterns of *tk* and *pol* mRNA accumulation were similar, although higher levels of *tk* transcripts were observed at early times and higher levels of *pol* transcripts were observed at late times. No new 5' termini were detected during the course of infection (Fig. 7). There was only a two- to threefold difference in the peak levels of *tk* and *pol* transcripts. Moreover, comparison of the areas under the curves shown in Fig. 8 indicated that the level of overall accumulation of *tk* mRNA was less than twofold greater than that of *pol* mRNA.

Relative distribution of *pol* transcripts on polyribosomes. To test the possibility that *pol* transcripts might be translated less efficiently than other HSV early mRNAs, we compared the polysome distribution profile of *pol* transcripts with that of transcripts for *dbp*. The lengths of the *dbp* transcript and its major open reading frame are similar to those of the *pol* transcript (14, 45). Therefore, assuming that elongation rates are similar, differences observed in the polysome distribution of these RNAs should be a reflection of differences in the efficiency of translation initiation.

Cytoplasmic supernatants prepared from cells infected for 5.5 h were fractionated by centrifugation through sucrose gradients. The distribution of RNA in such a gradient is shown in Fig. 9a, revealing a typical polysome profile. Fractions from the gradient shown in Fig. 9a were pooled as

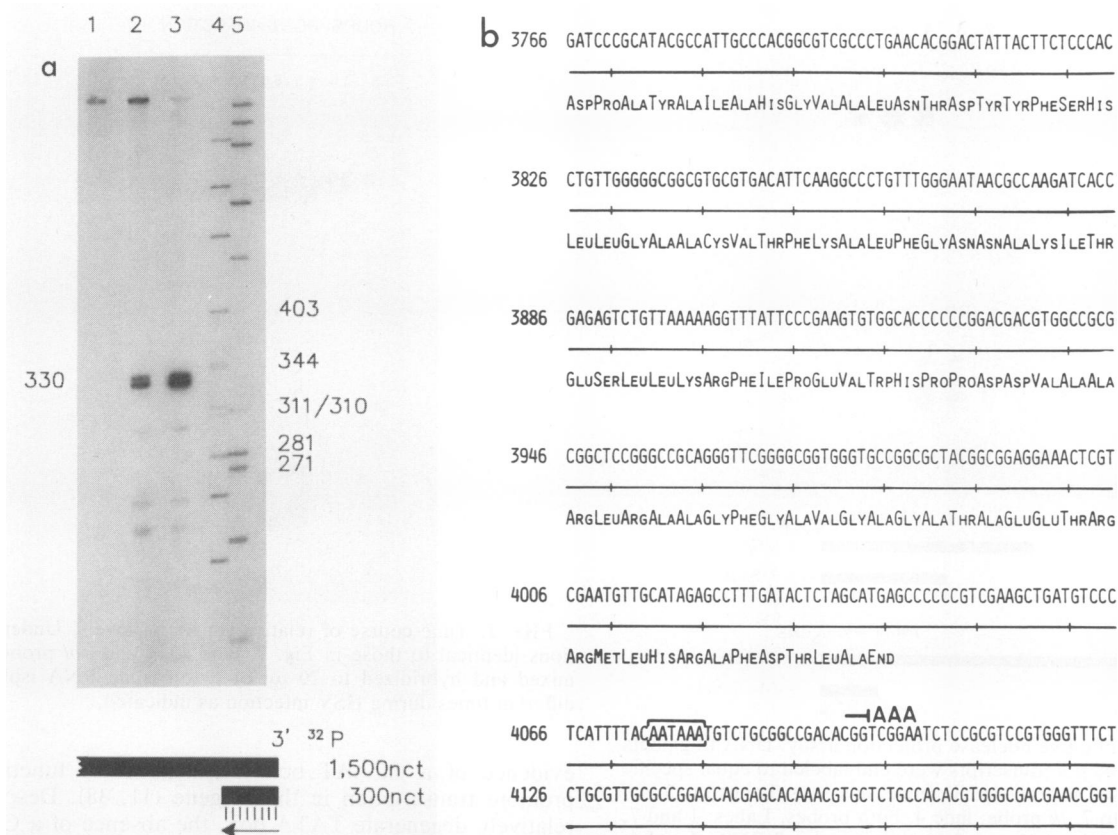


FIG. 5. Mapping of the polyadenylation site of the *pol* transcript. (a) S1 nuclease analysis with a DNA fragment 3'-end labeled at a *Bam*HI site (0.436) and extending approximately 1.5 kb to a *Sal*I site (0.445). Lane 1, S1-resistant products protected by 20 μ g of mock-infected-cell RNA; lane 2, products from 10 μ g of infected-cell RNA; lane 3, products from 20 μ g of infected-cell RNA; lane 4 and 5, pBR322 *Alu*-*Bam*HI and ϕ X174 *Hae*III markers, respectively. (b) Sequence from the *Bam*HI site at 0.436 to the *Kpn*I site at 0.439. The location of the major S1-sensitive site is shown juxtaposed between a consensus polyadenylation sequence (in brackets) and a G+T-rich region. These positions are shown along with the C terminus of the major *pol* open reading frame. Nucleotides are numbered from the center of the *ori*_L palindrome (14, 57).

indicated. Quantitative S1 nuclease analysis was performed with a mixture of the *Bam*HI-*Bst*EII *pol* probe used in Fig. 2b and 7 and the same fragment labeled at the 5' end at the *Bst*EII site to detect *dbp* transcripts (51). Control experiments similar to those shown in Fig. 6 were performed to ensure that this assay was both specific and quantitative (data not shown). This analysis revealed major differences in the polysome profiles of *pol* and *dbp* transcripts (Fig. 9b and c). The majority of *pol* transcripts, in contrast to *dbp* transcripts, were found within the slower-sedimenting fractions of the gradient, including free ribonucleoprotein, ribosomal subunits, monosomes, and small polysomes (pools A to G). Conversely, only a small proportion of *pol* transcripts and a majority of *dbp* transcripts were found to be associated with large polyribosomes (pools H to O). S1 analysis revealed no alterations in the 5' ends of *pol* transcripts associated with the various fractions.

Samples of the same pooled fractions bound to nitrocellulose were hybridized with uniformly labeled probes for *pol*, *dbp*, or *tk*. Using this procedure, we detected relative levels of *pol* and *dbp* transcripts in each fraction similar to those detected by the nuclease protection assay. Moreover, even though the length of *tk* coding sequences is only one-third that of *pol* coding sequences, there was still a much greater representation of *tk* transcripts on large polyribosomes than of *pol* transcripts (results not shown). These observations

suggest that at 5.5 h after infection, when levels of *pol* mRNA accumulation have nearly peaked, the translation of this mRNA is inefficient.

DISCUSSION

Structure of the major *pol* transcript. In this study we used S1 nuclease protection, primer extension assays, and exonuclease VII analysis to map the 5' end of the major *pol* transcript (Fig. 2 and 3). As shown in Fig. 10, we have assigned the location to two closely spaced sites 51 and 57 nucleotides to the left of the *Bam*HI site at 0.413. We chose this location, determined by S1 nuclease protection (Fig. 2b), rather than the location obtained by primer extension and exonuclease VII (Fig. 3a and b), because it was derived by direct comparison with a DNA sequence ladder of the probe. However, given the potential for S1 nuclease either to spare unpaired bases (e.g., Fig. 4) or to "nibble" into double-stranded regions, there may be an error of a few bases in either direction in our mapping.

Mapping of the polyadenylation site of the major *pol* transcript (Fig. 5), together with the mapping of its 5' end, predicts an unspliced, polyadenylated RNA molecule of 4.2 kb. This would be consistent with one of the two roughly equimolar *pol* mRNA species detected by Holland et al. (19) with Northern blot hybridization analysis. In similar exper-

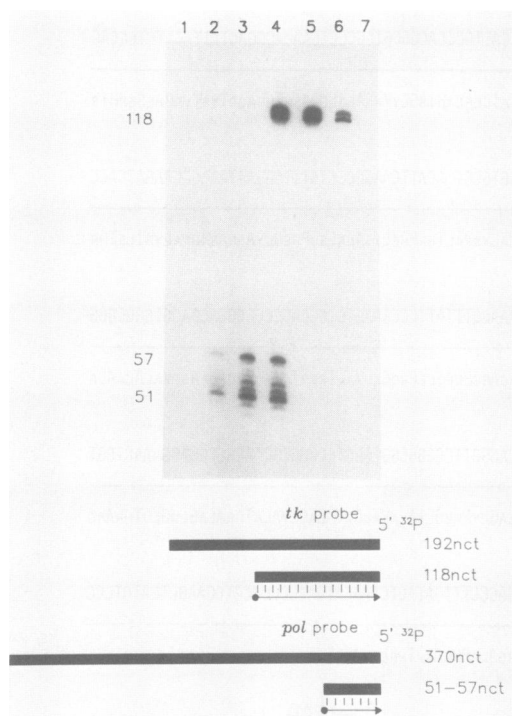


FIG. 6. Quantitative nuclease protection assay. DNA fragments specific for *tk* and *pol* transcripts were end labeled to equal specific activities and used as probes in S1 nuclease assays. Lanes 1 to 3, *pol* probe; lanes 5 to 7, *tk* probe; lane 4, both probes. Lanes: 1 and 7, products derived from 20 μ g of mock-infected-cell RNA; 2 and 6, products derived from 10 μ g of infected-cell (6 h) RNA; 3 to 5, products derived from 20 μ g of infected-cell RNA.

iments, Rafield and Knipe detected a single RNA species from this region (46). We and others have also been unable to distinguish more than one transcript by Northern blot analysis at various time postinfection (55; Yager and Coen, unpublished results). We find no evidence for major S1-sensitive sites within 375 nucleotides upstream (Fig. 4) or 500 nucleotides downstream (Fig. 2a) from the major 5' end. Nor can we detect such sites within 300 nucleotides upstream or 1,200 nucleotides downstream from the 3' end (Fig. 5). Thus, assuming that there are no internal splicing events, the major *pol* transcript contains the entire long open reading frame of the *pol* gene (14, 45). Preliminary results obtained from two-dimensional S1 nuclease mapping (data not shown) argue against the existence of any major *pol* transcripts generated by internal splices. Nevertheless, we cannot absolutely exclude the possibility that such splices exist, nor can we exclude the possibility that differences between our results and those of Holland et al. (19) are due to the different cell lines that were used by the different laboratories.

The *pol* promoter and *ori_L* palindrome. The sequences upstream from the 5' end of the *pol* transcript are similar to those of other viral early gene promoters. The sequence CATAA, roughly 24 nucleotides upstream from the *pol* transcript 5' end, probably serves as the TATA box (Fig. 10) (3). Further upstream, a G+C-rich region centered roughly 68 nucleotides upstream of the 5' end matches the consensus Sp1 decanucleotide binding site (5). This site is a transcriptional control signal in several genes (21, 23), and there are two such sequences in the HSV *tk* promoter, one on each strand, that affect its transcription (11, 22, 23, 38). There is no

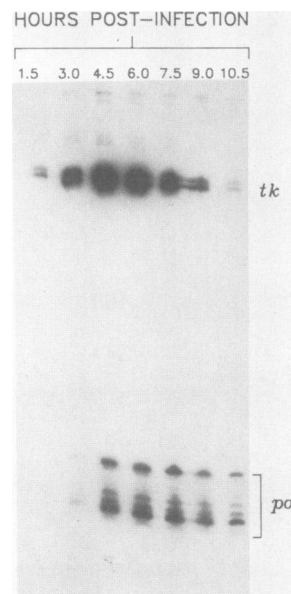


FIG. 7. Time course of relative transcript levels. Under conditions identical to those in Fig. 7, lane 4, *tk* and *pol* probes were mixed and hybridized to 20 μ g of cytoplasmic RNA isolated at different times during HSV infection as indicated.

evidence of a CCAAT box (3), which also functions to promote transcription in the *tk* gene (11, 38). Despite the relatively degenerate TATA box, the absence of a CCAAT box, and the presence of only one consensus Sp1 site, we observed that the accumulation levels of *pol* mRNA were similar to those of *tk* mRNA (Fig. 7 and 8). Similarly, nuclear runoff experiments have revealed that the rate of transcription of *pol* during HSV infection is comparable to that of *tk* (11, 55).

Both the Sp1 consensus sequence found upstream of the major *pol* transcript and the minor S1-protected products map within the 144-bp palindrome associated with *ori_L* of HSV. Origins of DNA synthesis frequently contain palindromic regions which are close to temporally regulated transcription units (6, 49, 57). Current evidence suggests that transcription factors or transcriptional activation of the DNA template may be required for the initiation of replication (12, 13, 21, 41).

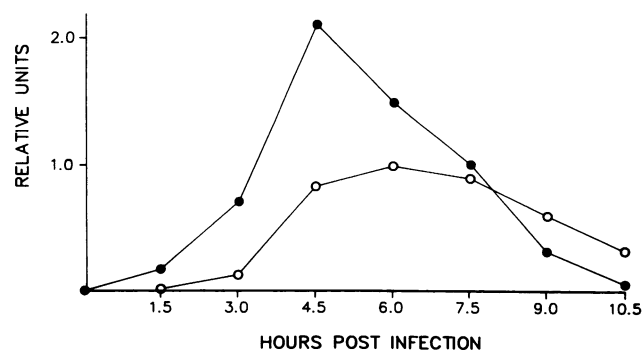


FIG. 8. Densitometric scan of quantitative nuclease protection assay. The results obtained by scanning an autoradiogram identical to the one in Fig. 7 but exposed for a shorter length of time so as to be in the linear range of the densitometer. Symbols: ●, *tk* probe; ○, *pol* probe.

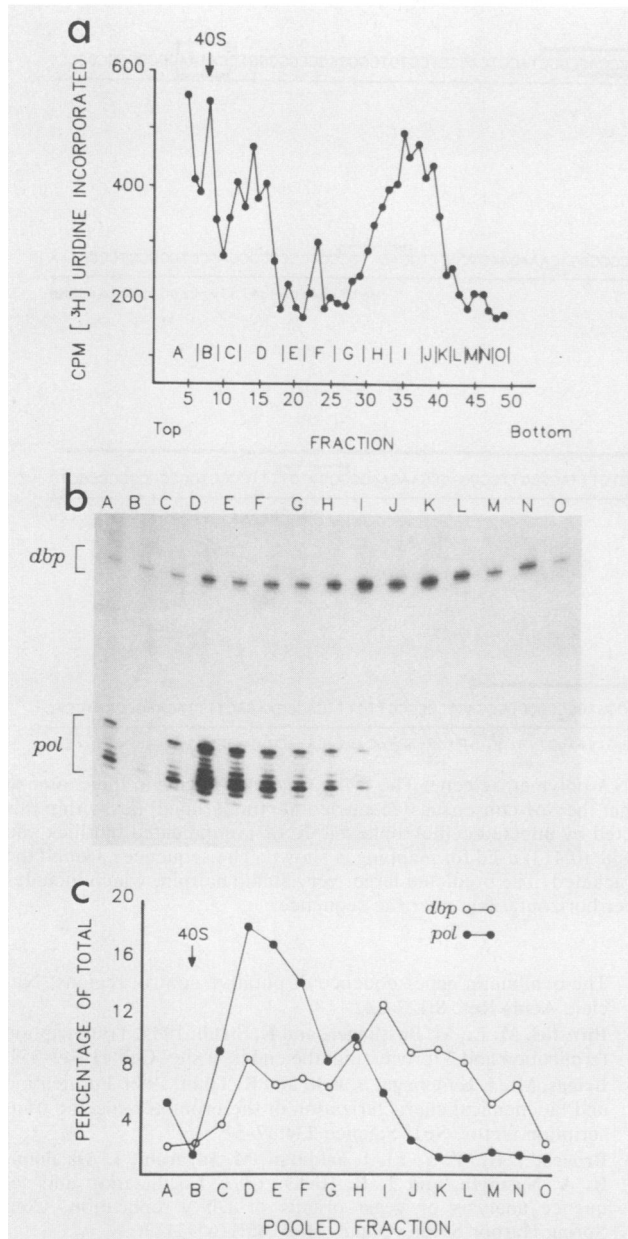


FIG. 9. Relative distribution of *pol* transcripts on polyribosomes. (a) Cytosols prepared from cells labeled with $[^3\text{H}]$ uridine and then infected for 5.5 h were fractionated by velocity sedimentation through sucrose gradients. Fractions were collected from the top, and the radioactivity in each was measured by scintillation counting. The position of the 40S peak was determined by ethidium bromide staining of portions fractionated by agarose gel electrophoresis. (b) Fractions pooled as indicated in panel a were used for quantitative nuclease protection analysis with *pol* and *dbp* probes. 5' ends of the *Bst*EII-*Bam*HI fragment were labeled to specific activities so that similar signals were obtained with unfractionated infected-cell RNA (not shown). (c) Graph of relative levels of *pol* and *dbp* transcripts in pooled fractions derived from densitometric scanning of the results in panel b.

Evidence that *pol* expression is inefficient at the level of translation. Selective translation of cellular as well as viral mRNAs has been described in several systems (1, 25, 26, 34), and various mechanisms have been proposed to account for this. For example, in adenovirus- and influenza virus-infected cells, translation of host mRNA is inhibited, appar-

ently at the level of both initiation and elongation (25, 26). In HSV-infected cells, it has been suggested from a comparison of overall polysome profiles and protein synthesis rates that transcripts can be found on inactive polysomes (47, 52).

The results presented here (Fig. 8 and 9) demonstrate that during the peak time of *pol* mRNA accumulation, relatively few *pol* transcripts were present on large polyribosomes. Thus, if *pol* expression is inefficient at the level of translation, it does not appear to be due to the presence of *pol* transcripts on inactive polysomes. Our results suggest instead that translation of *pol* transcripts is inefficient at the level of initiation. Alternatively, a very rapid rate of elongation relative to *dbp* and *tk* transcripts could explain the absence of *pol* mRNA on large polysomes. However, this is not consistent with the observed levels of synthesis and accumulation of the translation products of these mRNAs (16, 17; Yager and Coen, unpublished results). Antisera generated against *pol-lacZ* fusion proteins are currently being used to compare the levels of TK, DBP, and Pol synthesis.

Sequence features of *pol* possibly involved in regulation of translation efficiency. As can be seen in Fig. 10, a number of features of the *pol* transcript might participate in the regulation of its translation. The initiation codon of the major *pol* open reading frame is found in a context that differs from the consensus sequence motif CC(A/G)CCAUGG (29) only by replacing G with a U at the first nucleotide after the AUG. Such substitutions have been shown to decrease expression; however, such decreases are not drastic when there is an A or G three bases upstream of the AUG (29). The major *pol* open reading frame is preceded by a short open reading frame, which might result in reduced utilization of the major *pol* open reading frame (31). However, because the initiation codon of the upstream open reading frame is in a nonpreferred context, UGCACAUGC, and the downstream open reading frame begins at least 80 nucleotides downstream of the termination codon of the upstream reading frame (32), the presence of the upstream open reading frame may not play a major role in *pol* expression.

In contrast, computer modeling of the *pol* transcript predicts the formation of a hairpin extending from +155 to +308 (Fig. 10) (18). This hairpin, which would encompass the initiation codon of the major *pol* open reading frame, has a predicted Gibbs free energy of -71 kcal/mol. The inhibitory effect on translation resulting from the introduction of less stable hairpin structures into the leader regions of mRNAs has been demonstrated (30, 42). We suggest that this feature of the *pol* transcript contributes to decreasing *pol* expression and are currently testing this hypothesis.

The biological significance of the relatively low abundance of many replicative polymerases remains unclear. If polymerases were present in large amounts, they might inappropriately sequester other replication factors with which they interact, as has been suggested for vesicular stomatitis virus RNA polymerase (40). Assuming that maintaining a low level of Pol is important to HSV, there are at least two plausible reasons why control of HSV DNA *pol* expression at the level of translation might be valuable. First, induction of early viral mRNAs, including *pol*, at the appropriate time may require that they be transcribed at relatively similar levels. This would require that expression of *pol* be regulated posttranscriptionally to prevent its overexpression. In this scheme, decreasing *pol* expression by inefficient translation would be no more advantageous than other strategies, such as decreasing *pol* mRNA stability. Second, control at the level of translation may offer the advantage of finer temporal control of Pol expression. For example, *pol* mRNA might be

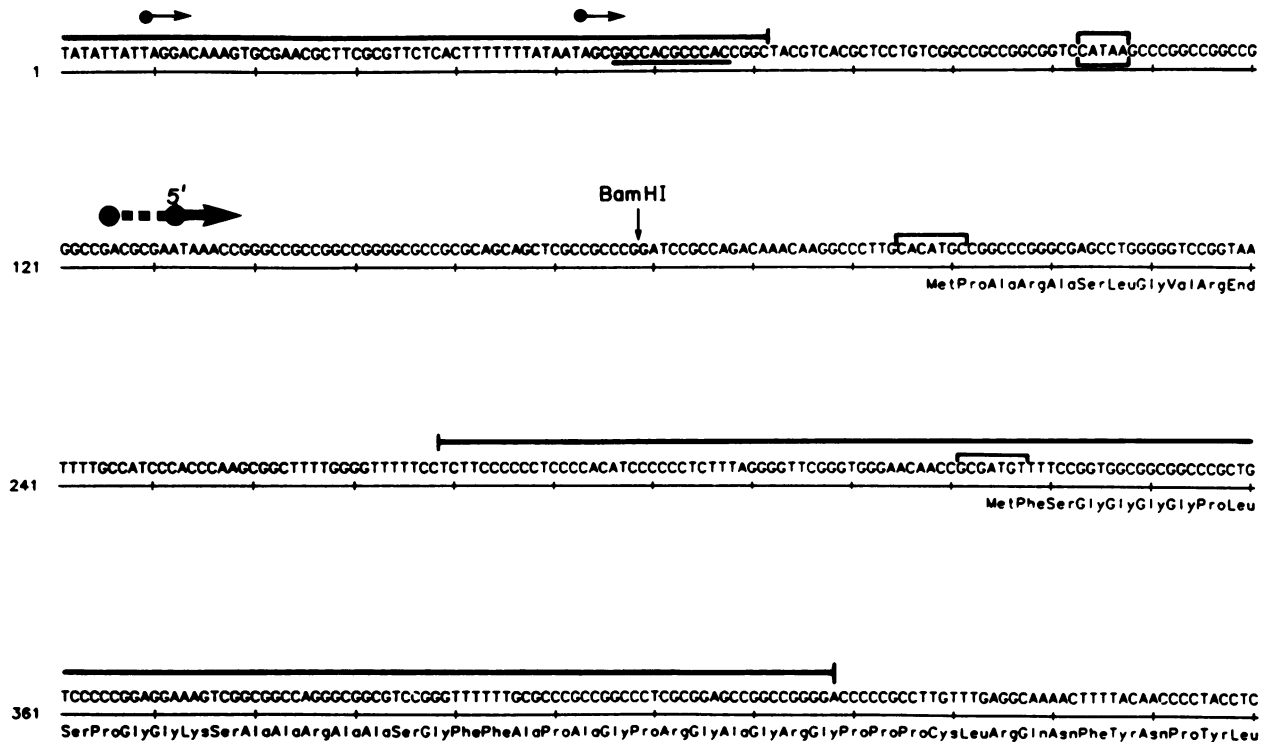


FIG. 10. Features of the DNA sequence in the 5' region of the HSV DNA polymerase gene. The DNA sequence begins in the center of the palindrome that contains *ori_L*, which is indicated by overlining. Note that the Sp1 consensus decanucleotide (underlined) lies within this palindrome. The positions of the major and minor S1-sensitive sites protected by infected-cell cytoplasmic RNA are indicated by thick and thin arrows, respectively. The candidate TATA box is boxed. The *Bam*HI site (0.413) used for mapping is shown. The sequences around the AUG of both the short upstream and the major open reading frames are bracketed. The predicted large, very stable hairpin, which includes the initiation codon for the long open reading frame, is indicated by another horizontal line over the sequence.

translated efficiently at early times but poorly at late times. Precedents for such temporal control have been reported for both the HSV system (20) and adenovirus (25, 26, 35, 53). Such control mechanisms may simply reflect preferential inhibition of translation of more poorly initiating mRNAs in the face of an overall decline in the efficiency of the translation machinery (34). The HSV system should be useful for exploring the biological significance of low polymerase expression and the mechanisms employed to achieve that end.

ACKNOWLEDGMENTS

We are grateful to R. M. Sandri-Goldin, M. Levine, and S. K. Weller for providing plasmids used in this study; K. Kerns and L. Leslie for technical assistance; J. Böni, A. Irmieri, D. Knipe, J. Miller, B. Roberts, and S. Weinheimer for critical comments; J. Scales and E. Zylstra for figure preparation; and S. L. McKnight for collaboration on the primer extension analysis.

This work was supported by Public Health Service research grant AI19838 from the National Institutes of Health and by the American Cancer Society (MV-242). D.R.Y. was supported by National Institutes of Health postdoctoral training grant T32 AI07245.

LITERATURE CITED

- Ballinger, D. G., and M. L. Pardue. 1983. The control of protein synthesis during heat shock in *Drosophila* cells involves altered polypeptide elongation rates. *Cell* 33:103-114.
- Banks, G. R., J. A. Boezi, and I. R. Lehman. 1979. A high molecular weight DNA polymerase from *Drosophila melanogaster* embryos. *J. Biol. Chem.* 254:9886-9892.
- Benoist, C., K. O'Hare, R. Breathnach, and P. Chambon. 1980. The ovalbumin gene-sequence of putative control regions. *Nucleic Acids Res.* 8:127-142.
- Birnstiel, M. L., M. Busslinger, and K. Strub. 1985. Transcription termination and 3' processing: the end is in site! *Cell* 41:349-359.
- Briggs, M., J. Kadonaga, S. Bell, and R. Tjian. 1986. Purification and biochemical characterization of the promoter-specific transcription factor, Sp1. *Science* 234:47-52.
- Broach, J. R., Y.-Y. Li, J. Feldman, M. Jayaram, J. Abraham, K. A. Nasmyth, and J. B. Hicks. 1982. Localization and sequence analysis of yeast origins of DNA replication. *Cold Spring Harbor Symp. Quant. Biol.* 45:1165-1173.
- Chartrand, P., C. S. Crumpacker, P. A. Schaffer, and N. M. Wilkie. 1980. Physical and genetic analysis of the herpes simplex virus DNA polymerase locus. *Virology* 103:311-326.
- Chartrand, P., N. D. Stow, M. C. Timbury, and N. M. Wilkie. 1979. Physical mapping of PAA^r mutations of herpes simplex virus type 1 and type 2 by intertypic marker rescue. *J. Virol.* 31:265-276.
- Chase, J. W., and C. C. Richardson. 1974. Exonuclease VII of *Escherichia coli*: mechanism of action. *J. Biol. Chem.* 249:4553-4561.
- Coen, D. M., D. P. Aschman, P. T. Gelep, M. J. Retondo, S. K. Weller, and P. A. Schaffer. 1984. Fine mapping and molecular cloning of mutations in the herpes simplex virus DNA polymerase locus. *J. Virol.* 49:236-247.
- Coen, D. M., S. P. Weinheimer, and S. L. McKnight. 1986. A genetic approach to promoter recognition during *trans* induction of viral gene expression. *Science* 234:53-59.
- de Villiers, J., W. Schaffner, C. Tyndall, S. Lupton, and R. Kamen. 1984. Polyomavirus DNA replication requires an enhancer. *Nature (London)* 312:242-246.
- Furth, M., M. Dove, and B. Meyer. 1982. Specificity determinants for bacteriophage lambda DNA replication. III. Activa-

- tion of replication in lambda ri^c mutants by transcription outside of *ori*. *J. Mol. Biol.* **154**:65–83.
14. **Gibbs, J. S., H. C. Chiou, J. D. Hall, D. W. Mount, M. J. Retondo, S. K. Weller, and D. M. Coen.** 1985. Sequence and mapping analyses of the herpes simplex virus DNA polymerase gene predict a C-terminal substrate binding domain. *Proc. Natl. Acad. Sci. USA* **82**:7969–7973.
 15. **Goldin, A. L., R. M. Sandri-Goldin, M. Levine, and J. C. Glorioso.** 1981. Cloning of herpes simplex virus type 1 sequences representing the whole genome. *J. Virol.* **38**:50–58.
 16. **Goldstein, D. J., and S. K. Weller.** 1988. Herpes simplex virus type 1-induced ribonucleotide reductase activity is dispensable for virus growth and DNA synthesis: isolation and characterization of an ICP6 *lacZ* insertion mutant. *J. Virol.* **62**:196–205.
 17. **Haar, L., and H. S. Marsden.** 1981. Two-dimensional gel analysis of HSV type 1-induced polypeptides and glycoprotein processing. *J. Gen. Virol.* **52**:77–92.
 18. **Hall, J., J. Gibbs, D. Coen, and D. Mount.** 1986. Structural organization and unusual codon usage in the DNA polymerase gene from herpes simplex virus type 1. *DNA* **5**:281–288.
 19. **Holland, L. E., R. M. Sandri-Goldin, A. L. Goldin, J. C. Glorioso, and M. Levine.** 1984. Transcriptional and genetic analyses of the herpes simplex virus type 1 genome: coordinates 0.29 to 0.45. *J. Virol.* **49**:947–959.
 20. **Johnson, D., and P. Spear.** 1984. Evidence for translational regulation of herpes simplex virus type 1 gD expression. *J. Virol.* **51**:389–394.
 21. **Jones, K. A., J. T. Kadonaga, P. J. Rosenfeld, T. J. Kelly, and R. Tjian.** 1987. A cellular DNA-binding protein that activates eukaryotic transcription and DNA replication. *Cell* **48**:79–89.
 22. **Jones, K. A., and R. Tjian.** 1985. Sp1 binds to promoter sequences and activates herpes simplex virus 'immediate-early' gene transcription *in vitro*. *Nature (London)* **317**:179–182.
 23. **Jones, K. A., K. R. Yamamoto, and R. Tjian.** 1985. Two distinct transcription factors bind to the HSV thymidine kinase promoter *in vitro*. *Cell* **42**:559–572.
 24. **Kadonaga, J. T., K. A. Jones, and R. Tjian.** 1986. Promoter-specific activation of RNA polymerase II transcription by Sp1. *Trends Biochem. Sci.* **11**:20–23.
 25. **Katze, M. G., D. DeCorato, and R. M. Krug.** 1986. Cellular mRNA translation is blocked at both initiation and elongation after infection by influenza virus or adenovirus. *J. Virol.* **60**:1027–1039.
 26. **Khalili, K., and R. Weinmann.** 1984. Shut-off of actin biosynthesis in adenovirus serotype-2-infected cells. *J. Mol. Biol.* **175**:453–468.
 27. **Knopf, K. W.** 1979. Properties of herpes simplex virus DNA polymerase and characterization of its associated exonuclease activity. *Eur. J. Biochem.* **98**:231–244.
 28. **Kornberg, A.** 1980. DNA replication. W. H. Freeman and Co., San Francisco.
 29. **Kozak, M.** 1984. Selection of initiation sites by eukaryotic ribosomes: effect of inserting AUG triplets upstream from the coding sequence for preproinsulin. *Nucleic Acids Res.* **12**:3873–3893.
 30. **Kozak, M.** 1986. Influences of mRNA secondary structure on initiation by eukaryotic ribosomes. *Proc. Natl. Acad. Sci. USA* **83**:2850–2854.
 31. **Kozak, M.** 1986. Selection of translational start sites in eukaryotic mRNAs, p. 35–41. *In* M. Mathews (ed.), *Current communications in molecular biology: translational control*. Cold Spring Harbor Laboratory, Cold Spring Harbor, N.Y.
 32. **Kozak, M.** 1987. Effects of intercistronic length on the efficiency of reinitiation by eucaryotic ribosomes. *Mol. Cell. Biol.* **7**:3438–3445.
 33. **Lee, M. Y. W. T., and N. L. Toomey.** 1987. Human placental DNA polymerase δ : identification of a 170-kilodalton polypeptide by activity staining and immunoblotting. *Biochemistry* **26**:1076–1085.
 34. **Lodish, H. F.** 1974. Model for the regulation of mRNA translation applied to haemoglobin synthesis. *Nature (London)* **251**:385–388.
 35. **Logan, J., and T. Shenk.** 1984. Adenovirus tripartite leader sequence enhances translation of mRNAs late after infection. *Proc. Natl. Acad. Sci. USA* **81**:3655–3659.
 36. **Maniatis, T., E. F. Fritsch, and J. Sambrook.** 1982. *Molecular cloning: a laboratory manual*. Cold Spring Harbor Laboratory, Cold Spring Harbor, N.Y.
 37. **Maxam, A., and W. Gilbert.** 1980. Sequencing end-labeled DNA with base-specific chemical cleavages. *Methods Enzymol.* **65**:499–560.
 38. **McKnight, S. L., R. C. Kingsbury, A. Spence, and M. Smith.** 1984. The distal transcription signals of the herpesvirus TK gene share a common hexanucleotide control sequence. *Cell* **37**:253–262.
 39. **McLaughlan, J., D. Gaffrey, J. L. Whitton, and J. B. Clements.** 1985. The consensus sequence YGTGTTY located downstream from the AATAAA signal is required for efficient formation of mRNA 3' termini. *Nucleic Acids Res.* **13**:1342–1369.
 40. **Meier, L., G. G. Harmison, and M. Schubert.** 1987. Homotypic and heterotypic exclusion of vesicular stomatitis virus replication by high levels of recombinant polymerase protein L. *J. Virol.* **61**:3133–3142.
 41. **Orr-Weaver, T., and A. Spradling.** 1986. *Drosophila* chorion gene amplification requires an upstream region regulating $\text{s}18$ transcription. *Mol. Cell. Biol.* **6**:4624–4633.
 42. **Pelletier, J., and N. Sonenberg.** 1985. Insertion mutagenesis to increase secondary structure within the 5' noncoding region of a eukaryotic mRNA reduces translational efficiency. *Cell* **40**:515–526.
 43. **Powell, K., and D. Purifoy.** 1977. Nonstructural proteins of herpes simplex virus. I. Purification of the induced DNA polymerase. *J. Virol.* **24**:618–624.
 44. **Proudfoot, N., and G. Brownlee.** 1976. 3' Non-coding region sequences in eukaryotic mRNA. *Nature (London)* **263**:211–214.
 45. **Quinn, J. P., and D. J. McGeoch.** 1985. DNA sequence of the region in the genome of herpes simplex virus type 1 containing the genes for DNA polymerase and the major DNA-binding protein. *Nucleic Acids Res.* **13**:8143–8163.
 46. **Rafield, L. F., and D. M. Knipe.** 1984. Characterization of the major mRNAs transcribed from the genes for glycoprotein B and DNA-binding protein ICP8 of herpes simplex virus type 1. *J. Virol.* **49**:960–969.
 47. **Silverstein, S., and D. L. Engelhardt.** 1979. Alterations in the protein synthetic apparatus of cells infected with herpes simplex virus. *Virology* **95**:334–342.
 48. **Smith, K. O.** 1964. Relationships between the envelope and the infectivity of herpes simplex virus. *Proc. Soc. Exp. Biol. Med.* **115**:814–816.
 49. **Stenlund, A., G. L. Bream, and M. R. Botchan.** 1987. A promoter with an internal regulatory domain is part of the origin of replication in BPV-1. *Science* **236**:1666–1671.
 50. **Stillman, B. W., F. Tamanoi, and M. B. Mathews.** 1982. Purification of an adenovirus-coded DNA polymerase that is required for initiation of DNA replication. *Cell* **31**:613–623.
 51. **Su, L., and D. M. Knipe.** 1986. Mapping of the transcriptional initiation site of the herpes simplex virus type 1 ICP8 gene in infected and transfected cells. *J. Virol.* **61**:615–620.
 52. **Sydiskis, R. J., and B. Roizman.** 1966. Polysomes and protein synthesis in cells infected with a DNA virus. *Science* **153**:76–78.
 53. **Thummel, C., R. Tjian, S. Hu, and T. Grodzicker.** 1983. Translational control of SV40 T antigen expressed from the adenovirus late promoter. *Cell* **33**:455–464.
 54. **Wagner, M. J., J. A. Sharp, and W. C. Summers.** 1981. Nucleotide sequence of the thymidine kinase gene of herpes simplex virus type 1. *Proc. Natl. Acad. Sci. USA* **78**:1441–1445.
 55. **Weinheimer, S., and S. L. McKnight.** 1987. Transcriptional and post-transcriptional controls establish the cascade of herpes simplex virus protein synthesis. *J. Mol. Biol.* **195**:819–833.
 56. **Weller, S. K., D. P. Aschman, W. R. Sacks, D. M. Coen, and P. A. Schaffer.** 1983. Genetic analysis of temperature-sensitive mutants of HSV-1: the combined use of complementation and physical mapping for cistron assignment. *Virology* **130**:290–305.
 57. **Weller, S. K., A. Spadaro, J. E. Schaffer, A. W. Murray, A. M. Maxam, and P. A. Schaffer.** 1985. Cloning, sequencing, and functional analysis of *ori_L*, a herpes simplex virus type 1 origin of DNA synthesis. *Mol. Cell. Biol.* **5**:930–942.